Savannah River National Laboratory®

A U.S. DEPARTMENT OF ENERGY NATIONAL LAB • SAVANNAH RIVER SITE • AIKEN, SC • USA

Mark-18A Loading Capacity and Dilute Acid Rinse of DGA Resin

M. S. Mills

S. Uba

April 2024

SRNL-STI-2024-00057, Revision 0

DISCLAIMER

Printed in the United States of America

Prepared for
U.S. Department of Energy

SRNL-STI-2024-00057
Revision 0

Keywords: *Actinide, Lanthanide, Separations*

Retention: *Lifetime*

Mark-18A Loading Capacity and Dilute Acid Rinse of DGA Resin

M. S. Mills
S. Uba

April 2024

Savannah River National Laboratory is operated by Battelle Savannah River Alliance for the U.S. Department of Energy under Contract No. 89303321CEM000080.

REVIEWS AND APPROVALS

AUTHORS:

M. S. Mills, Separations & Actinide Science Date

S. Uba, Nuclear Detection and Forensics Date

TECHNICAL REVIEW:

W. D. King, Separations Sciences & Engineering, Reviewed per E7 2.60 Date

APPROVAL:

J. M. Duffey, Manager Date
Separations & Actinide Science

G. A. Morgan, Manager Date
Separations Sciences & Engineering

C. R. Armstrong, Mark-18A Program Manager Date

ACKNOWLEDGEMENTS

Eddie Kyser is acknowledged for his technical insight and assistance in planning and executing the experiment.

This work was funded by the National Nuclear Security Administration's Office of Environment, Safety, and Health (NA-ESH).

EXECUTIVE SUMMARY

Savannah River National Laboratory is developing a separations flowsheet for the recovery of valuable elements from irradiated ^{242}Pu targets. The primary impetus for this effort is to recover the rich amount of ^{244}Pu contained in the targets, however, the targets also contain other valuable isotopes such as heavy Cm and $^{241,243}Am$. DGA Resin, developed by Eichrom Technologies Inc., was selected to recover these materials from the 7 – 9 M HNO_3 matrix raffinate of the anion exchange process used to separate Pu. The resin has a high affinity for trivalent actinides and rare earth elements (REEs) in moderate to strong nitric acid. After loading the resin, the extracted materials (including Cm and Am) are to be recovered as oxides in a two-step process by thermally drying and reducing the mass and volume of the resin in the process column followed by calcination of the resultant residue. It is desirable to reduce the amount of residual HNO_3 in the resin bed prior to these furnace operations, but the reduced acid concentration is known to lower the distribution coefficients of the components of interest to the extractant. The purpose of this study was to validate the loading capacity of the resin and determine losses to be expected from rinsing the loaded resin with dilute HNO_3.

A non-radiological simulant was developed and pumped through a column containing DGA Resin using similar operating parameters to be used for the process. Sm and Nd were used as surrogates to represent Cm and Am, respectively. The resin was intentionally loaded beyond saturation from the 7.51 M HNO_3 feed simulant to determine the saturation capacity, washed with fresh 8 M HNO_3, and rinsed with 0.26 M HNO_3. A loading profile was developed, and the resin was determined to have a trivalent metal saturation capacity of 74 µmol/mL resin. However, the post-8 M HNO_3 wash trivalent metal capacity of 68 µmol/mL resin represents the practical capacity of the resin for the Mark-18A process. Lighter lanthanides breakthrough the resin well before the saturation capacity is reached. Breakthrough of ~1% of cumulative Nd fed to the column occurred with cumulative REE retention on the resin of 58 µmol (8.5 mg)/mL resin at 17.8 bed volumes (BV) of feed processed. This is lower than reported in a previous SRNL DGA loading study, which stated that Nd broke through at 11 mg REE, Am, and Zr/mL resin. After transferring 22.2 BV of feed through the column, similar to the estimated process feed volume, 0% of Sm and 6% of Nd broke through the resin bed.

Rinsing the saturated resin bed with 0.26 M HNO_3 was found to result in a rapid reduction in retention of REEs by the resin. After processing 2.8 BV of dilute acid rinse, the mean resin bed free acid concentration was reduced to 0.28 M and 3.1 BV of dilute acid rinse resulted in a reduction of the cumulative REE retention to 52 µmol/mL of resin. It is desired to minimize losses to no more than 5% of the maximum amount of Cm contained in any quarter Mk-18A target. Estimating Cm and Am losses from the dilute acid rinse based on Sm and Nd losses, respectively, predicts that Cm and Am losses will be significant with excessive dilute acid rinse. Additionally, Sm may be more strongly retained by the resin than Cm, indicating that this approach could underpredict Cm losses. Based on Sm and Nd retention, it is estimated that 1.2 BV of dilute acid rinse would result in losses of 4.8% and 4.2% of the maximum amount of Cm and Am contained in a quarter target from saturated resin, respectively, and a mean resin bed free acid concentration of 1.8 M. Due to the non-conservative nature of this approach, 1 BV of dilute acid rinse may be a more appropriate target. With 1 BV of dilute acid rinse, it is estimated that Cm and Am losses would be 3.1% and 2.9% of the maximum amount contained in a quarter target from saturated resin, respectively, with a mean resin bed free acid concentration of 3.0 M. Recycle of the rinse effluent to the DGA feed tank is recommended so that it can be reprocessed with the next quarter target to further reduce losses.

TABLE OF CONTENTS

LIST OF TABLES

LIST OF FIGURES

LIST OF ABBREVIATIONS

ACS	American Chemical Society
BV	Bed volume
DGA	Diglycolamide
DI	Deionized
ICP-MS	Inductively coupled plasma mass spectrometry
ID	Inner diameter
Mk-18A	Mark-18A
ORNL	Oak Ridge National Laboratory
PMMA	Polymethyl methacrylate
REE	Rare earth element
SRNL	Savannah River National Laboratory
SRS	Savannah River Site
TODGA	*N,N,N',N'*-tetra-n-octyldiglycolamide

1.0 Introduction

Savannah River National Laboratory (SRNL) is developing a separations flowsheet to recover rare and highly valued isotopes from sixty-five irradiated Mark-18A (Mk-18A) targets at the Savannah River Site (SRS). These targets were originally loaded with up to nominally 120 g of elemental Pu, consisting of >98 atom percent ^{242}Pu and irradiated in SRS's K-Reactor from 1969 to 1979 under high neutron flux of up to 10^{15} neutrons cm^{-2} s^{-1}. The original purpose of the Mk-18A targets was to produce heavy Cm, defined as containing ≥50% ^{246}Cm, as ^{252}Cf feedstock.[1] Twenty-one of the original 86 targets were processed at Oak Ridge National Laboratory's (ORNL) Radiochemical Engineering Development Center from 1972 to 1973 for this purpose.[1, 2] The present interest in the Mk-18A targets and the impetus for SRNL's extensive process development effort is their uniquely high composition of ^{244}Pu. Plutonium-244 is the longest lived isotope of Pu with a half-life of 81 million years and has value as a standard reference material for fundamental studies of Pu and for the production of superheavy elements.[2, 3] The United States Government's current inventory of usable ^{244}Pu is about 300 mg, and the remaining Mk-18A targets are estimated to contain up to nominally 20 g of ^{244}Pu.[3] Additionally, the targets contain other valuable isotopes, including hundreds of grams of heavy Cm and tens of grams of ^{241}Am and ^{243}Am which are available for recovery from these targets.

The Mk-18A separations flowsheet includes a caustic dissolution of the target's aluminum cladding. The majority of the target material, including the actinides, lanthanides (Ln), and other fission products, are insoluble in the caustic media. The undissolved solids are filtered and dissolved in 7 - 9 M HNO_3 at or near boiling. Pu is recovered from the solution by anion exchange via Reillex HPQ resin packed in a continuous flow column. The Reillex resin has a high affinity for tetravalent actinides (e.g., Pu(IV), Np(IV)), which load onto the resin as a hexanitrato complex from a high nitrate solution matrix.[4, 5] The dissolved Cm, Am, and Ln are in the trivalent state and are rejected to the Reillex raffinate along with the remaining fission products.[6]

N,N,N',N'-tetra-n-octyldiglycolamide (TODGA) was selected to recover the Cm and Am from the anion exchange raffinate. The extractant is produced as a solid resin by Eichrom Technologies Inc. under the trade name of DGA Resin. The resin is composed of 40 wt.% TODGA physisorbed onto a polymethyl methacrylate (PMMA) support structure, representing the balance of the resin mass. TODGA extracts trivalent actinides and rare earth elements (REE) from nitric acid solutions and generally has a low affinity for non-REE transition metals with some exceptions.[7-9] The final form of the Cm and Am material will be an oxide. Both the TODGA and PMMA components of the resin are composed of only C, H, O, and N (CHON) atoms, and are thus completely incinerable.[10, 11] This property is leveraged to convert these metals from nitrate complexes sorbed to DGA resin to oxides via a two-step process in which the loaded resin is dried and thermally decomposed (i.e., reduced in both mass and volume) in the same process column in which it is loaded followed by calcination of the resultant residue.[12] The decomposition process occurs under reduced oxygen conditions with argon while the resultant residue is calcined in air.

The baseline flowsheet was to perform the decomposition process with the resin under the same 7 – 9 M HNO_3 conditions from which it was loaded followed by washing with fresh acid of similar concentration to displace the feed.[12, 13] With the baseline equipment design configuration, reduced oxygen conditions were initially promoted by the radial diffusion of argon in the headspace of the column during furnace operations. The process was developed and demonstrated near full-scale in a laboratory study.[12] However, there were challenges with the validation of the decomposition process at full scale with the actual process equipment. Several full-scale tests were conducted in an attempt to validate a heating profile based on laboratory results, but an acceptable material product was difficult to achieve with the baseline design configuration. Furthermore, during a December 2022 test, an exothermic reaction occurred at or near the surface of the resin resulting in unexpected smoke and low intensity flames at a relatively low operating temperature.[14] It

was concluded that the exothermic reaction was the result of air in-leakage during a process intended to be inert. However, this behavior was likely exacerbated by the relatively high concentration (nominally 7 M) and volume of entrained nitric acid, a strong oxidant, in the resin bed. Additionally, there is evidence that, under certain conditions, the decomposition temperature of DGA is significantly reduced in the presence of nitric acid.[15] Following the December 2022 test, several process modifications were proposed for testing. The key modifications include the displacement of the 7 – 9 M nitric acid from the resin bed prior to furnace operations and the active flow of argon up through the resin bed during the decomposition step rather than diffusion in the column headspace.[14]

While it is desirable to reduce the amount and concentration of nitric acid in the resin bed prior to furnace operations, it was acknowledged that this could result in product losses. Eichrom's data indicate that the distribution coefficient for Am(III), a primary target product along with Cm, decreases with decreasing nitric acid concentration.[9] Cm is anticipated to have a stronger affinity for DGA Resin than Am.[8] Distribution coefficients reported for the extraction of Am and Cm using dissolved TODGA in organic liquids from a nitric acid solution indicate that Cm has a higher affinity for TODGA than Am and the distribution coefficient trends are similar and proportional to the nitric acid concentration.[16] However, past SRNL experience has indicated that eluting from DGA Resin with dilute nitric acid (e.g., pH 2) is challenging.[17] This is believed to be due to the difficulty in completely displacing the nitric acid to levels less than 0.1 M. Furthermore, Eichrom recommends stripping actinides from the resin with dilute HCl solutions rather than HNO_3, indicating the inefficiency of eluting with dilute HNO_3.

The purpose of this study was to quantify potential losses from the displacement of the 7 – 9 M HNO_3 from the resin bed prior to decomposition furnace operations.[18] Additionally, the process knowledge has significantly developed since the last Mark-18A DGA study.[13] A loading profile was characterized with a more representative feed simulant and loading conditions than was utilized in previous studies.

2.0 Experimental Procedure

I-grade DGA Resin – Normal of 300 – 840 μm bead size was used for this study. The resin was wetted in 8 M HNO_3 for several hours, filtered, and placed in 0.35 M HNO_3 for several days. The resin-acid slurry was then packed in a 1.5 × 30 cm Econo-Column Bio-Rad chromatography column and the resin bed topped with a glass frit. Support at the top of the resin bed is necessary because the resin is buoyant in 8 M HNO_3. Details are provided in Table 2-1 below. Note that DGA Resin swells upon hydration, and the swelling has been observed to be proportional to the acid concentration. The bed volume (BV) shown in Table 2-1 was obtained by measuring the height of the resin bed after packing the resin slurry in the 1.5 cm ID column and allowing to settle. DGA Resin is not buoyant in 0.35 M HNO_3. The initial height of the resin bed was marked on the glass column, and it was not observed to vary during or several days after the experiment.

Table 2-1. Resin preparation details

Dry resin volume (mL)	34 ± 0.5
Resin mass[(a)] (g)	15.0616
8 M HNO_3 wetting solution (mL)	98.8
0.35 M HNO_3 wetting solution (mL)	98.2
Resin height in column (cm)	24.2
Bed volume (BV) (mL)	42.8

(a) Resin mass as received.

A feed simulant was prepared targeting the composition described by Mills et al.[18] by dissolving metal nitrates in deionized (DI) H_2O, adding concentrated ACS reagent grade HNO_3 targeting a final concentration of 8 M, and diluting to volume with DI H_2O in a volumetric flask. Sm and Nd were used as surrogates for Cm and Am, respectively, based on their similar distribution coefficient profiles for liquid DGA in solvent extraction systems.[7, 16] Both Sm and Nd are present in the Mk-18A targets. The simulant

Sm and Nd concentrations were increased relative to the anticipated concentrations for these species to represent the sum of Sm and Cm and the sum of Nd and Am concentrations, respectively, on a mole basis. The feed was analyzed for metals by inductively coupled plasma mass spectrometry (ICP-MS) and for free acid by acid-base titration. All ICP-MS and free acid titration values for this work are reported with relative standard deviation (RSD) uncertainties of up to 10% and 5%, respectively. The composition of the feed based on analysis is provided in Table 2-2 below.

Table 2-2. DGA feed simulant composition

Component	Source	Concentration
Fe (µM)	$Fe(NO_3)_3•9H_2O$	4.69×10^3
Cu (µM)	$Cu(NO_3)_2•3H_2O$	4.03×10^2
Sr (µM)	$Sr(NO_3)_2$	5.74×10^1
Y (µM)	$Y(NO_3)_3•6H_2O$	4.86×10^1
La (µM)	$La(NO_3)_3•6H_2O$	2.20×10^2
Ce (µM)	$Ce(NO_3)_3•6H_2O$	6.58×10^2
Pr (µM)	$Pr(NO_3)_3•6H_2O$	1.62×10^2
Nd[a] (µM)	$Nd(NO_3)_3•6H_2O$	1.17×10^3
Sm[b] (µM)	$Sm(NO_3)_3•6H_2O$	8.23×10^2
Eu (µM)	$Eu(NO_3)_3•5H_2O$	1.78×10^1
Gd (µM)	$Gd(NO_3)_3•6H_2O$	3.49×10^2
Tb (µM)	$Tb(NO_3)_3•6H_2O$	2.28×10^1
Dy (µM)	$Dy(NO_3)_3•xH_2O$	1.69×10^1
Ho (µM)	$Ho(NO_3)_3•5H_2O$	6.51×10^0
Er[c] (µM)	Impurity	4.68×10^0
Tm[c] (µM)	Impurity	1.55×10^{-2}
Yb[c] (µM)	Impurity	4.11×10^{-1}
Lu[c] (µM)	Impurity	3.86×10^{-2}
Sum of REEs (µM)	-	3.52×10^3
HNO_3 (M)	ACS reagent grade HNO_3	7.51×10^0

a. 93.6 mol% represents Nd, 6.4 mol% represents Am.
b. 16.1 mol% represents Sm, 83.9 mol% represents Cm.
c. Not specifically added to simulant but identified by ICP-MS. Likely impurities in other REE nitrate salts.

Solutions were pumped to the packed column via a Masterflex C/L Microflex peristaltic pump. The raffinate from the column was plumbed to flow through a 90-mm custom SRNL design flow cell like that used in the Mk-18A process in the Shielded Cells Facility. Column effluents were collected in tared polyethylene bottles. A photo of the experimental configuration is provided in Figure 2-1 below.

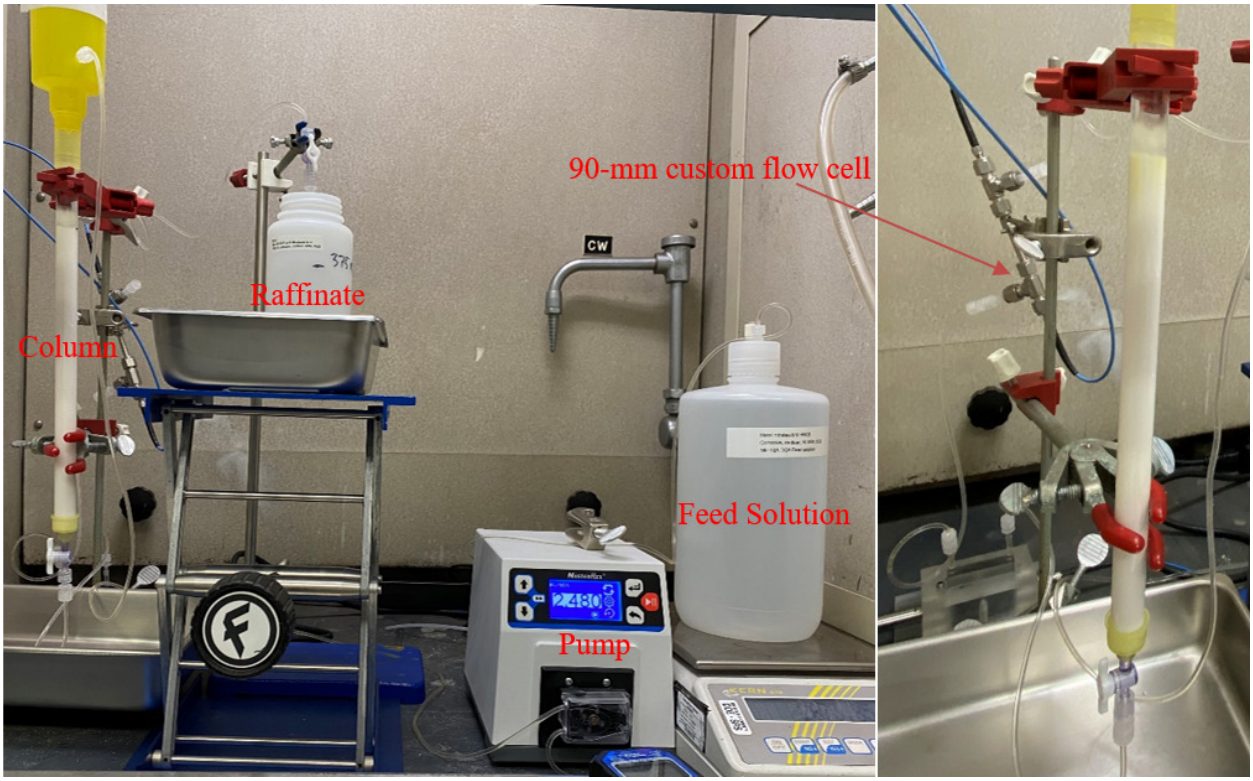

Figure 2-1. Experimental configuration

The resin was conditioned with 8 M HNO_3, loaded with the feed described in Table 2-2, washed with fresh 8 M HNO_3, and rinsed with 0.26 M HNO_3 with the following parameters.[a] An HNO_3 concentration of 0.35 M was targeted for the rinse solution, as this is the target concentration of dilute acid available in the Mk-18A process. The difference in these concentrations is not expected to impact the conclusions of this work. The resin was intentionally saturated and loaded beyond the previously reported capacity to determine the bounding losses from a dilute acid rinse for conservatism. The column operating parameters for this experiment are provided in Table 2-3 below. The experiment was performed at ambient laboratory temperature, which typically ranges from approximately 18.5 to 22 °C.

Table 2-3. Column operating parameters

Step	Volume (BV)[a]	Average volumetric rate (BV h^{-1})	Average linear velocity (cm min^{-1})	Average REE flow rate (µmol cm^{-2} min^{-1})
Condition with 8 M HNO_3	4.50	6.26	2.52	-
Load	33.2	3.23	1.30	4.60
Wash with 8 M HNO_3	1.92	7.79	3.14	-
Rinse with 0.26 M HNO_3	3.24	6.66	2.68	-

[a] "BV" is bed volume and represents a volume of solution equivalent to the volume of the packed resin bed.

[a] Condition/wash acid concentration calculated based on final volume and concentrated acid volume and molarity. Rinse acid concentration measured by free acid titration.

The effluent composites were weighed, sampled, and the density was measured. Samples of all effluent composite solutions, except the condition solution, were analyzed for metals by ICP-MS. Additionally, the dilute acid rinse composites were analyzed for free acid.

Spectrophotometric measurements were performed with a tungsten-halogen and xenon-arc flash lamp as light source, delivered via optical fiber cables to the custom designed flow cell. This flow cell was assembled from commercial-off-the-shelf (COTS) components and transmitted light intensities were measured using an Avantes Multichannel Spectrometer, AVS-RACKMOUNT-USB2. The optical system is described in detail in Appendix A. Real-time monitoring of the DGA column effluent was performed with a 90.01 ± 0.01 mm flow cell shown in Figure 2-1 and Figure 2-2, positioned and plumbed to promote a vertical up flow fluid processing direction. Transmitted light intensities of a collimated light beam from the flow cell were measured and interpreted by an Avantes spectrometer. The spectrometer was configured in a custom dual-beam diode array design and transmitted light intensities were measured by reference and sample detectors within an Avantes Multichannel Spectrometer. Light was integrated over 10 ms and 500 spectra were averaged by the spectrometer before passing the data to the control software to provide an average spectrum over approximately 5 second intervals. Absorbance values were calculated, and spectra were interpolated to a standardized set of wavelengths from 200 – 900 nm with 0.2 nm resolution using the instrument control software.[19] The absorbance values were calculated using equation *(1)*, where A = absorbance, I = transmitted light, and I_0 = incident light. The final absorbance spectrum is calculated by subtracting from the blank absorbance spectrum.

$$A = -\log_{10}\left(I/I_0\right) \qquad (1)$$

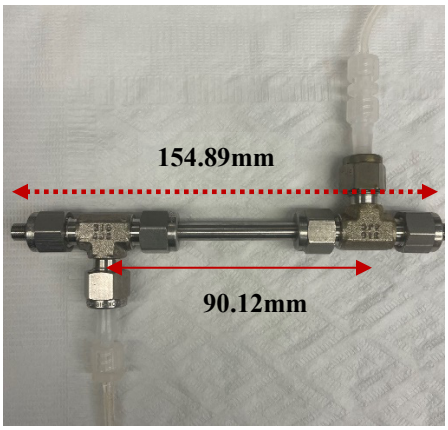

Figure 2-2. Stainless steel flow cell

2.2 Quality Assurance

Requirements for performing reviews of technical reports and the extent of review are established in manual E7 2.60. SRNL documents the extent and type of review using the SRNL Technical Report Design Checklist contained in WSRC-IM-2002-00011, Rev. 2.

3.0 Results and Discussion

3.1 Loading

The average effluent composition, measured by ICP-MS, is shown in Figure 3-1 below. The measured composite concentration represents the average for each cut and is shown at the cumulative volumetric midpoint. Composite effluent compositions are provided in Appendix A.

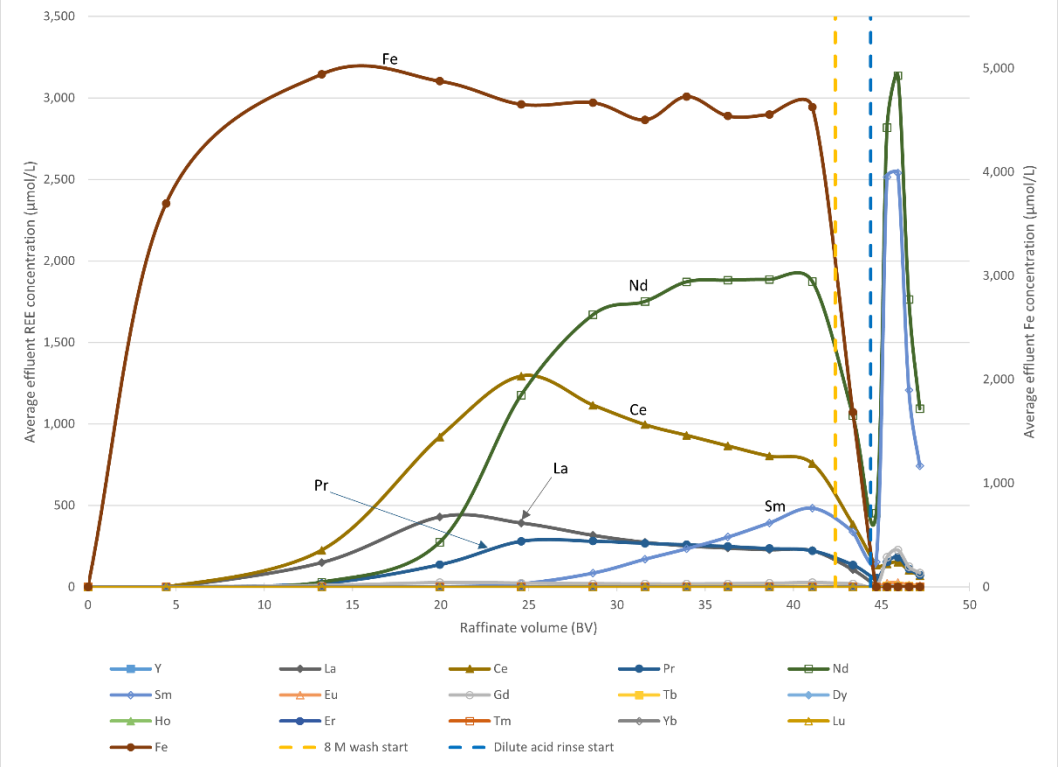

Figure 3-1. Average effluent composition

The column loading profile, calculated based on the cumulative solution volume processed, the known feed concentrations, and the measured effluent concentrations, is shown in Figure 3-2. The resin has a REE capacity of up to 68 µmol/mL resin (~10 g of REEs/L resin) during loading with the feed simulant under these experimental conditions. This is determined by the maximum cumulative REE retention, which remains essentially constant once reached. Additionally, 6 µmol of Fe/mL resin is retained in the resin bed once the capacity is reached for an overall trivalent metal capacity of 74 µmol/mL resin during loading. Upon washing the resin bed with ~2 BV of fresh 8 M HNO_3, the REE and Fe retention drops to 64 and 4 µmol/mL resin, respectively, with an overall trivalent metal retention of 68 µmol/mL resin. The capacity reduction is due to the displacement of unextracted interstitial feed components and slight leaching of the saturated resin. Thus, this represents a practical capacity of the resin under the processing conditions of interest.

The resin capacity determined in this study is within the range of those reported in the literature. Horwitz et al. reported that the TODGA resin capacity is 77 µmol Eu/mL of resin bed in a slurry-packed column when loaded from a 0.0274 M Eu and 4.0 M HNO_3 feed.[9] The same paper states that the resin capacity is approximately 86 µmol Eu/mL of resin bed. Eichrom's website states that the DGA Resin functional capacity (i.e., with minimal breakthrough) is 7-8 mg Eu (46-53 µmol)/mL of resin.[20] The feed composition significantly influences retention. Distribution from the aqueous phase to TODGA increases with nitric acid concentration. A feed with a higher concentration of REEs and actinides is expected to have greater retention on the resin up to the maximum resin capacity limit (corresponding to loading and saturation of all available TODGA sorption sites) due to the increased driving force for mass transfer. For example, the Eu feed in Horwitz's study that resulted in a TODGA resin capacity of 77 µmol Eu/mL of resin bed is an order of magnitude higher than the REE concentration of the simulant for this study.[9]

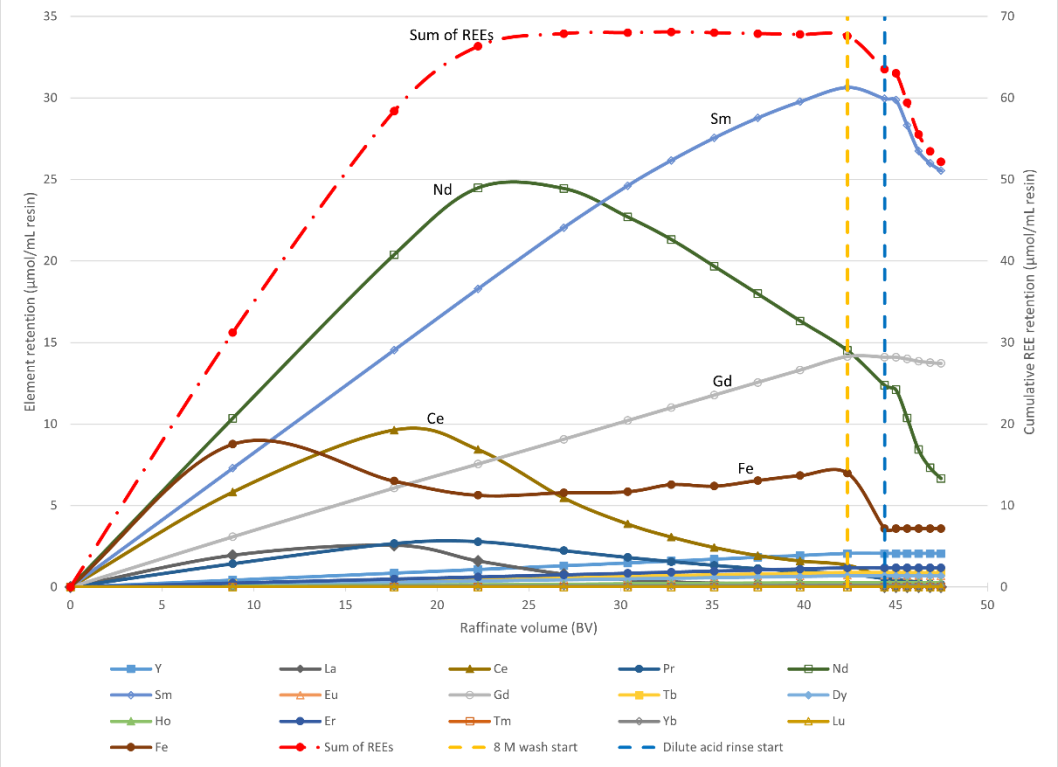

Figure 3-2. Resin loading profile

Another metric for comparing the resin capacities is the stoichiometric capacity of TODGA. Horwitz et al. measured a TODGA to Eu mole ratio of 3.19:1 with the resin and concluded that this represents a TODGA to trivalent cation stoichiometry of 3:1.[9] This is consistent with the TODGA stoichiometry determined from a liquid-liquid extraction system with an aqueous solution of Nd and 3 M HNO_3.[21] Assuming the DGA Resin is 40 wt.% of 94% pure TODGA,[9] the TODGA to retained REE ratio measured in this work is 3.4:1 prior to the 8 M HNO_3 wash and 3.6:1 after the wash. Including Fe, the TODGA:trivalent metal ratio is 3.1:1 prior to the 8 M HNO_3 wash and 3.4:1 after the wash. Slight differences in resin capacities could be due to inefficiencies associated with the larger I-grade resin (300 – 840 µm) relative to the more common analytical DGA Resin (50 - 100 µm) or the lower REE feed concentration of the feed in this study.

With this feed composition, Nd initially loads on the DGA Resin at the highest concentration of all measured species followed by Fe, Sm, Ce, and Gd, respectively. As the resin sites approach saturation, lighter lanthanides are displaced in favor of heavier ones. Nd displacement by more strongly retained REEs (indicated by a hump in the loading profile in Figure 3-2) from the resin occurs as the resin approaches saturation with REEs. Nd displacement is preceded by the displacement of Ce and La. This is further illustrated in Figure 3-3. Fe is weakly retained by the resin, initially loading at 8.8 µmol/mL resin after processing 8.9 BV of feed. However, as more feed is processed through the column, Fe is partially displaced from the resin until a steady retention of nominally 6 µmol/mL resin is reached. The initial displacement of Fe is represented by an increase in the effluent concentration to above the feed concentration. Within 27 BV processed, the effluent Fe concentration settles to within ± 3% of the feed concentration. Fe is more concentrated than any other feed component by at least a factor of 4 and the Fe feed concentration is 33% higher than the sum of REEs. The high concentration of Fe in the feed likely results in a much higher retention than would be achieved with a feed concentration comparable to other components. The loading profile in Figure 3-2 also demonstrates that there are significant losses from rinsing the saturated resin bed

with dilute HNO_3, as indicated by decreased element and cumulative REE capacities and an increase in effluent concentrations. This is discussed in more detail below.

The percent retention of the REEs on the DGA Resin with respect to the amount fed through the column is shown in Figure 3-3. Elements are labeled with their atomic number. Figure 3-3 illustrates that 100% of the REEs are initially retained by the DGA Resin up to at least 46% of the measured resin capacity in this study. However, once the resin is loaded to 86% capacity, the retention of low atomic number lanthanides is rapidly reduced, and breakthrough occurs. La through Nd successively breakthrough the column in order of increasing atomic number between 8.8 and 17.6 BV of feed with cumulative REEs retained on the resin between 31 and 58 μmol (4.5 and 8.5 mg)/mL resin, respectively. This is consistent with data provided by Horwitz et al., which indicate that TODGA resin selectivity for lanthanides increases with increasing atomic number. Their data also show that the relationship between resin selectivity and atomic number is logarithmic with more significant differences in selectivity at lower atomic numbers.[9] Horwitz et al.'s data were developed from batch contacts of resin with three stock solutions containing five to six REEs. The ratio of the elements to each other in these solutions is not clear. At atomic numbers greater than 60 (Nd), there are several differences in the trends observed in data developed in this study and that provided by Horwitz et al. For example, Sm (Z=62) is initially retained more than Gd (Z=64), Tb (Z=65), and Dy (Z=66). However, once the resin is saturated, the retention of Sm drops significantly in favor of higher atomic number elements. Similarly, Eu (Z=63) has a higher retention throughout loading than Gd, Tb, and Dy. The initial strong retention of Sm over Gd, Tb, and Dy could be due to the significantly higher concentration of Sm in the feed. However, the feed concentrations of Eu, Tb, and Dy are similar and the Gd feed concentration is an order of magnitude higher than Eu. Another difference in this data and that from the batch contacts in Horwitz et al.'s study is the retention of Y. Horwitz et al. found that the TODGA resin selectivity for Y is between Gd and Tb while the resin has a higher selectivity for lanthanides of atomic numbers greater than 65 than Y. The data developed in this study indicate that Y is the most strongly retained REE in the feed matrix with 100% retention during loading and minimal losses from resin washing and rinsing. Varying absorption and desorption kinetics of these species likely contributed to differences in element retentions in this study, with a dynamic flow column, and the batch contact data from Horwitz et al.

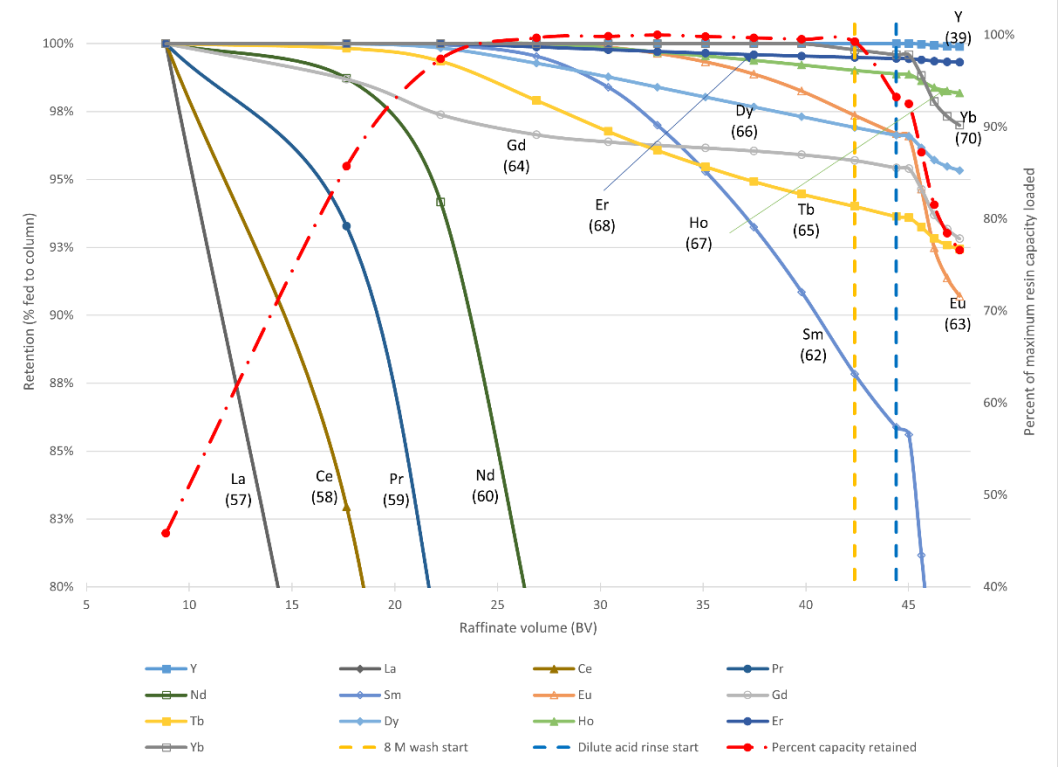

Figure 3-3. Element retention on DGA resin

A previous SRNL DGA loading study for Mk-18A reported that Nd breakthrough occurred with the resin loaded to 11 mg/mL resin with a similar feed matrix.[8] The process column was designed based on this metric, assuming 80% efficiency. The present study demonstrated that breakthrough occurs significantly earlier. In McCann et al.'s study, the 11 mg/mL resin breakthrough point was first identified with their "simulant 1", which was at least 7 times more concentrated than the anticipated feed concentration. They performed another experiment with "simulant 2", which was more dilute. The feed compositions between the experiment in the present study and the McCann simulant 2 experiment were generally similar (element concentrations within ± 40%). Two notable exceptions are that McCann et al.'s simulant 2 Sm and Fe concentrations were 235% and 41% of the concentrations used in this study, respectively. McCann et al. stated that Nd began to breakthrough when the resin was loaded with simulant 2 to 11 mg REE, Am, and Zr/mL resin, as they predicted from results with a more concentrated simulant. However, there is ambiguity regarding the resin bed volume in the McCann experiment, used to calculate breakthrough capacity. In McCann et al.'s paper, the simulant 2 column is described as 2.2 × 20.3 cm with 77 mL of DGA Resin. However, in McCann's SRNL Electronic Laboratory Notebook for their simulant 2 experiment, the column is described as 2 cm ID packed to 20.3 cm with DGA Resin for 64 mL resin bed volume.[22] If the loading of 11 mg REE, Am, and Zr/mL resin was calculated with a resin volume of 64 mL but the actual resin volume was 77 mL, then the loading at breakthrough would be 9.1 mg REE, Am, and Zr/mL resin, which is in reasonable agreement with the results of this study with 99% of Nd retained by the resin when loaded to 8.5 mg REE/mL resin.

If the breakthrough point for McCann et al.'s simulant 2 was correctly identified, the difference could be related, in part, to differences in flowrates and linear velocities in the present study and that used by McCann et al. The flowrates and linear velocities were 3.23 BV/h and 1.30 cm/min in this experiment and 2.6 BV/h and 0.89 cm/min in the McCann experiment, respectively. The loading rate for the 2.374" ID Mk-18A process DGA column is planned to be between 0.88 to 1.40 cm/min.[18] Flowrate is inversely proportional to

the residence time and linear velocity is inversely proportional to the time that the feed solution is in contact with a length of resin bed. The two parameters are similar, but both are important. Linear velocity is of particular importance because its inverse represents a kinetic limitation for cations to interact with discrete TODGA sites.

Figure 3-4 shows the effluent concentrations represented as a percent of the feed concentration at the volumetric midpoint for each cut. It illustrates the complex chromatographic behavior of these components in the presence of DGA Resin. The plot demonstrates that the effluent concentrations of lighter lanthanides, particularly La, Ce, Pr, and Nd, are initially non-detectable but that as more feed is processed, they evolve to significantly greater than the feed concentration. This is a result of these elements being displaced from the TODGA sites by more strongly retained components. By 42 BV of feed processed, the effluent concentration of La was 102% of its feed concentration, indicating that it had essentially been completely displaced from the resin. Extrapolating the data, it is clear that Ce and Pr would follow suit with further processing. While Nd is also displaced from the TODGA sites by other components, its effluent concentration did not reach a peak followed by approaching the feed concentration like La, Ce, and Pr. Rather, the effluent concentration of Nd settles to 160% of the feed concentration between 35 to 42 BV of feed processed. This indicates that while Nd is displaced by more strongly retained components, Nd itself continued to displace La, Ce, and Pr. With further processing, the concentration of Nd would eventually approach 100% of the feed concentration as well.

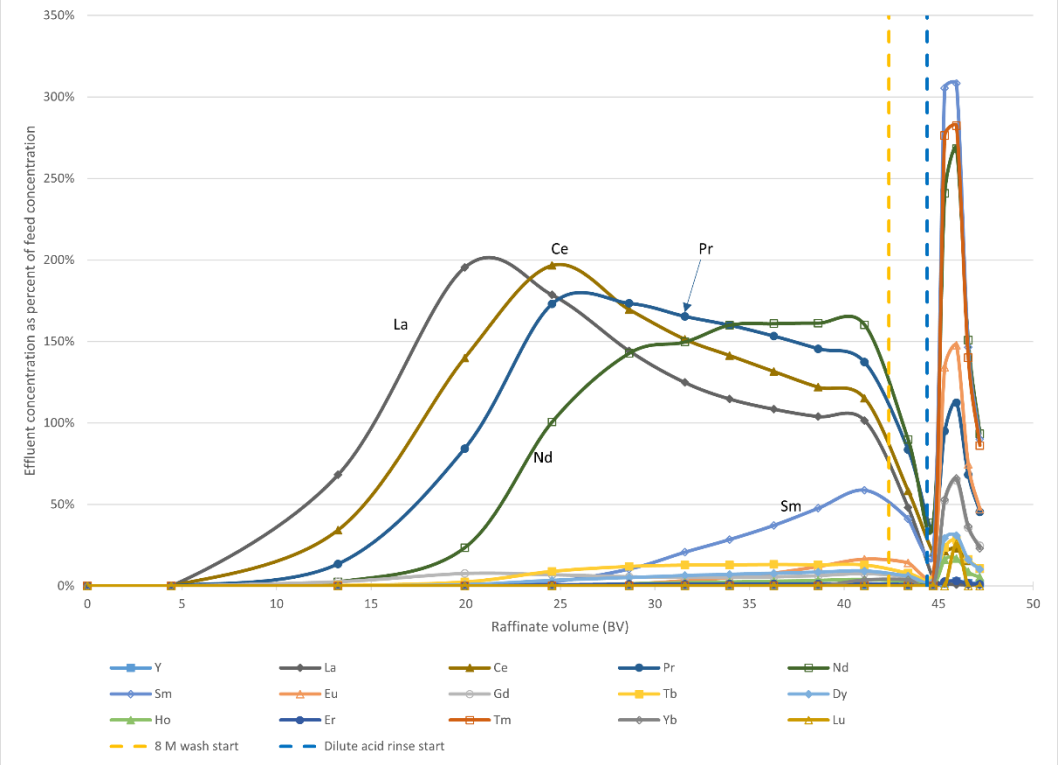

Figure 3-4. Effluent concentration as a percent of feed concentration

Of particular interest in this study is the retention of Sm and Nd, which are present in the targets but also used as surrogates for Cm and Am, respectively. The volume of a quarter target batch of Mk-18A DGA feed is estimated to be equivalent to 22 BV of the nominally 750-mL DGA column.[18] In the current study after processing 22.2 BV the resin was loaded with REEs to 66 µmol/mL resin (97% capacity), and 0% of Sm and 6% of Nd had broken through the resin bed. Cm and Am are represented as 83.9% and 6.4% of the

Sm and Nd in the feed simulant, respectively. Thus, if these are perfect surrogates, 0% of Cm and 0.4% of Am are predicted to breakthrough with the richest quarter target during loading.

Figure 3-5 shows the real time effluent absorption spectra evolution during the loading and fresh 8 M HNO_3 wash phases of the experiment. The absorption band centered at *ca* 393 nm is the most intense and represents ferric nitrate.[23] Iron is weakly retained by the resin and has no value to the program so the high absorbance is an inconvenient feature, but its development does provide some insight to early loading behavior. Particularly, when the absorbance representing Fe at *ca* 393 nm increases to greater than the absorbance in the feed, which represents displacement of Fe from the resin by more strongly retained REEs. At ~11 BV, absorption bands representing Nd developed at *ca* 578 nm, 739 nm, and 791 nm.[8, 24, 25] As Nd continued to breakthrough the resin and the effluent concentration increased, the absorbance at these wavelengths grew significantly and further absorption bands representing Nd developed at *ca* 510 nm, 523 nm, and 867 nm, by ~25 BV of feed. Shortly after beginning the fresh 8 M HNO_3 wash, the band centered at *ca* 393 nm, representing Fe, was eliminated while the bands representing Nd approached a constant value. This is due to the displacement of interstitial feed from the resin bed. While the absorption band for Fe centered at *ca* 393 nm was eliminated, absorption bands became distinguishable centered at *ca* 370 nm and *ca* 402 nm. These bands are attributed to Sm and were not distinguishable during loading, despite the increasing effluent Sm concentration as loading progressed.[24, 26] This is likely due to interference from the high absorption at *ca* 393 nm representing Fe. Thus, Sm cannot be relied upon as an indicator of breakthrough for Cm in this matrix in the presence of Fe. The development of absorption bands representing Fe and Nd in the effluent during loading are consistent with average concentrations measured by ICP-MS, shown in Figure 3-1. The presence of the Nd bands in the raffinate provide a warning of forthcoming breakthrough of Cm or Am during actual Mk-18 processing. The most distinguishable Nd absorption occurs at *ca* 578 nm. Light absorption at this wavelength should be monitored to predict potential breakthrough.

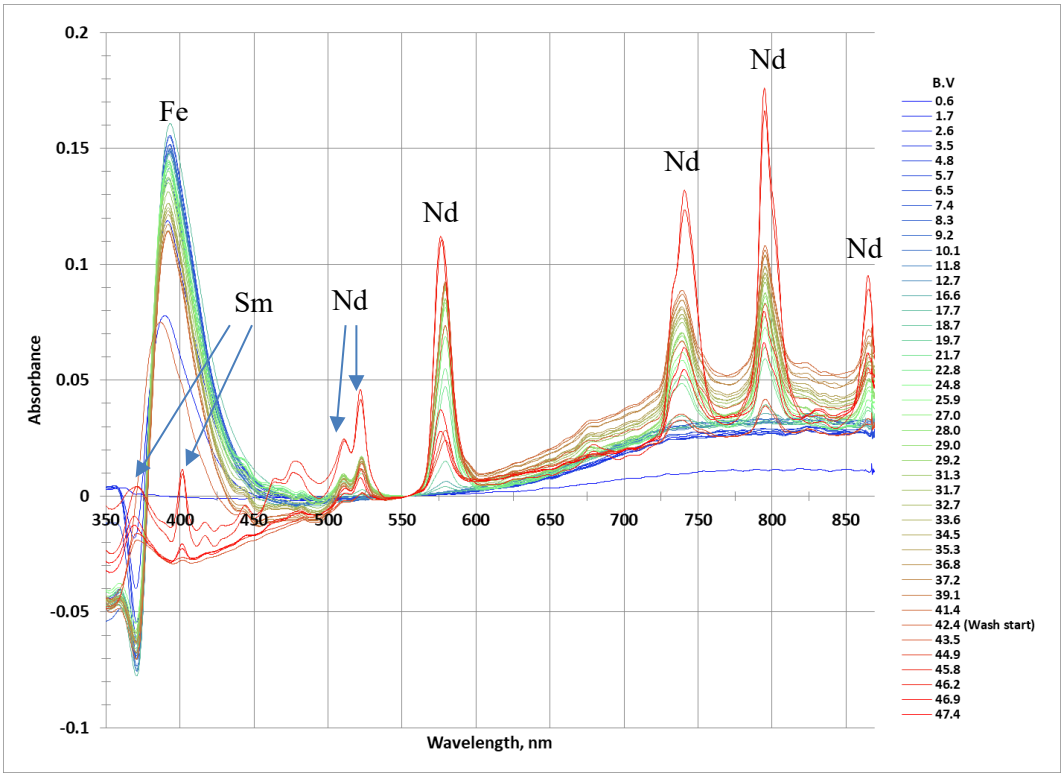

Figure 3-5. Absorption spectral evolution during loading and 8 M HNO_3 wash

3.2 Dilute Acid Displacement

A primary objective of this study was to determine the losses from loaded DGA Resin from rinsing the resin bed with dilute nitric acid to reduce the column nitrate concentration prior to furnace operations. The resin was intentionally saturated to determine bounding losses. Figure 3-2 and Figure 3-3 demonstrate that there is a reduction in the retention of REEs to 77% of the maximum resin capacity obtained during loading from 3.1 BV of dilute acid rinse. The resin loading and acid profiles during the wash and rinse are provided in Figure 3-6 (focused on this processing period from). The mean free acid concentration was reduced from 7.5 M to 0.28 M after processing 2.8 BV of 0.26 M HNO_3 through the column. The cumulative REE retention on the resin was reduced to 52 µmol/mL of resin with 3.1 BV of total dilute acid rinse. Extrapolating the data, further but diminishing losses would be realized with additional rinsing of the resin bed.

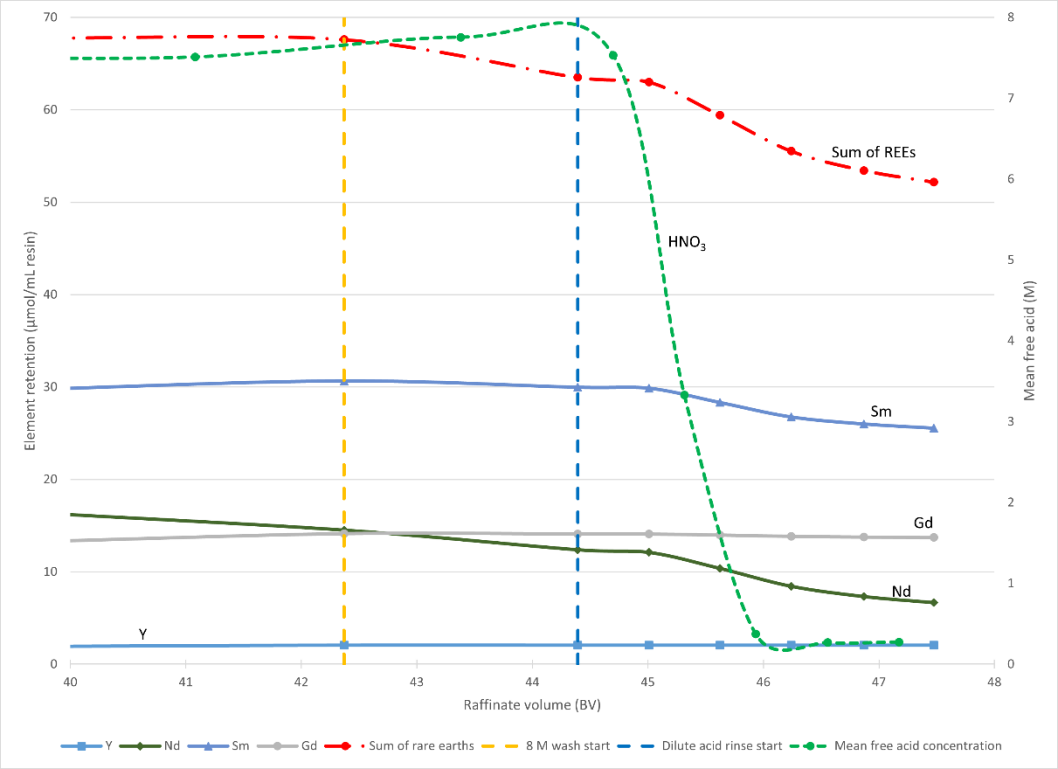

Figure 3-6. DGA retention and acid profile during resin bed wash and rinse

Figure 3-7 shows REE retention on the resin through the dilute acid rinse relative to the pre-rinse loading (0 BV corresponds to beginning of dilute acid rinse). It illustrates that Pr, Ce, and Nd experience the most significant reduction in retention by the resin during the dilute acid rinse. La was already completely displaced from the resin by other REEs prior to the rinse. Similar to the loading behavior where these lower atomic number lanthanides were displaced from the resin by heavier ones, they are also the most readily eluted from the resin under dilute acid conditions. There is less than a 3% reduction in the retention of Gd and heavier lanthanides from 3.1 BV of dilute acid rinse, except Tm, which is reduced by 11% of its pre-rinse concentration. Samarium, as a surrogate for Cm, exhibits a moderate reduction in retention of 15% with 3.1 BV of rinse.

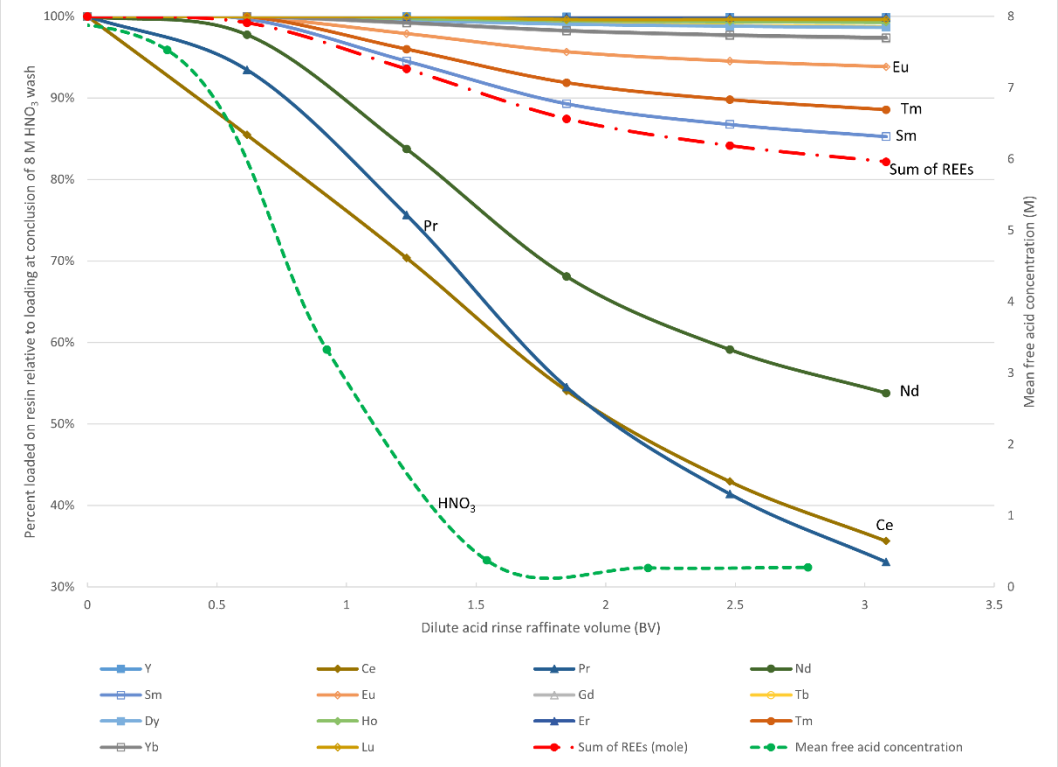

Figure 3-7. Resin retention from dilute acid rinse

Losses of Cm and Am relative to the maximum amount contained in a quarter Mk-18A target are of interest to the program. Losses of no more than 5% of these values are targeted. The maximum amount of Cm and Am predicted in 25% of any target is 3.24 g and 0.33 g, respectively.[27] The predicted losses of Cm and Am, assuming that they are represented by 83.9% and 6.4% of the Sm and Nd, respectively, relative to these maximum target values are provided in Figure 3-8. This analysis predicts Cm and Am losses to be significant based on measured Sm and Nd retention during this experiment, respectively. There is a substantial amount of Cm contained in the Mk-18A targets, which is represented by the majority of Sm in this experiment's simulant. There is far less Am contained in the targets but its surrogate, Nd, is retained less strongly than the Cm surrogate, Sm. Cm and Am losses are predicted to be 4.8% and 4.2% of the maximum amount contained in a quarter target from 1.2 BV of dilute acid rinse based on Sm and Nd losses in this experiment, respectively. This rinse volume is interpolated to provide a resin bed HNO_3 concentration of 1.8 M. As a contingency to ensure no more than 5% of the Cm or Am is lost, 1 BV of rinse may be an appropriate target. This would result in predicted losses of 3.1% and 2.9% of the maximum amount of Cm and Am contained in a quarter target, respectively, and a resin bed HNO_3 concentration of 3.0 M. It is emphasized that the desorption kinetics of Cm and Am under dynamic column flow conditions during loaded resin rinsing with dilute acid have not been tested and may differ from the desorption kinetics of their respective surrogates, Sm and Nd. Recycle of the column rinse effluent to the DGA feed tank is recommended so that this solution can be reprocessed with the next quarter target batch to further reduce Am/Cm losses.

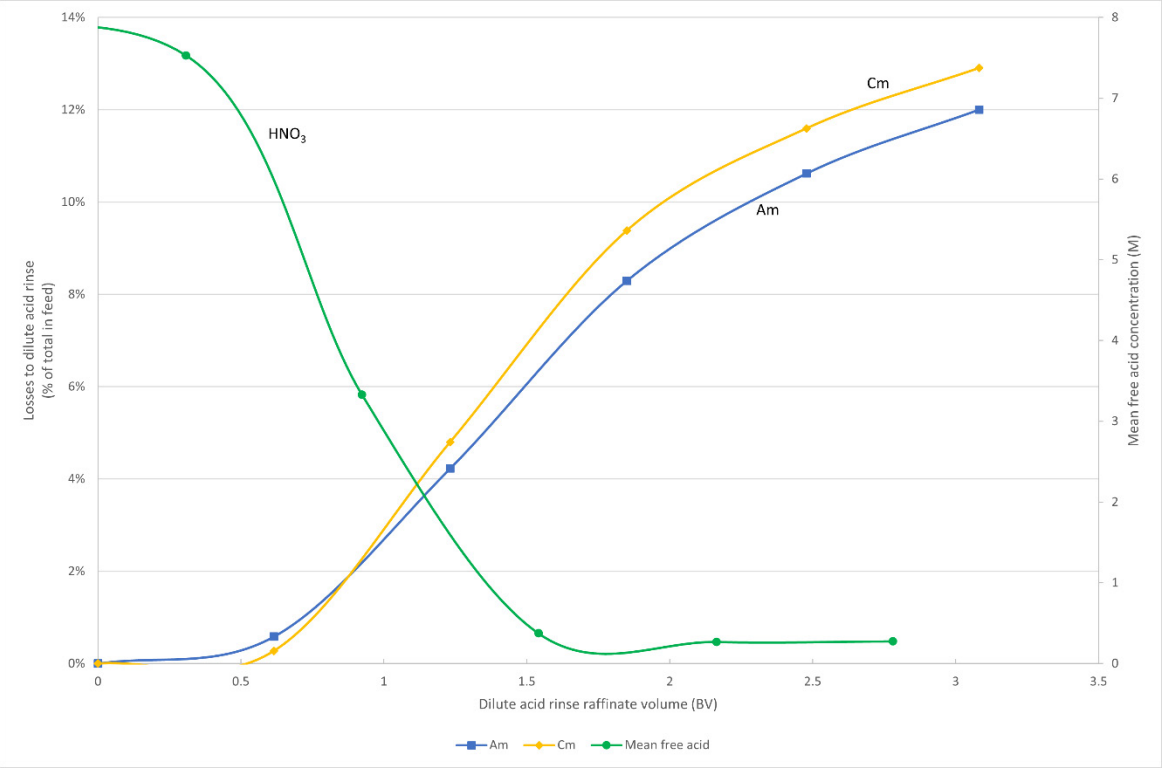

Figure 3-8. Predicted losses of Cm and Am from dilute acid rinse

In this experiment, the resin was loaded significantly beyond what is predicted for Shielded Cells operations. Thus, these loss predictions are conservative if Sm and Nd are conservative surrogates for Cm and Am. In this context, a conservative surrogate is one with less affinity for the extractant and would therefore desorb or be displaced from the resin more readily. Data provided by Zhu et al. for a 0.1 M TODGA/*n*-dodecane system and various concentrations of aqueous nitric acid indicate that the distribution coefficients for Am are similar to those for Nd but slightly higher, indicating Nd is a conservative surrogate.[7] This is consistent with data presented by Geist et al. for a 0.2 M TODGA/5% 1-octanol in TPH.[28] However, both Zhu and Geist indicate that the distribution coefficient for Sm is slightly higher than Cm across the range of nitric acid concentrations evaluated. Thus, in those solvent extraction systems, Sm has a stronger retention by TODGA than Cm. Extraction behavior on DGA Resin generally follows similar trends as dissolved TODGA in a solvent extraction system.[9] Thus, Cm losses from the dilute acid rinse would likely be higher than predicted from Sm losses in this non-radiological experiment based on this data.

Real time UV-vis measurements were also recorded during the dilute acid rinse phase of the experiment. These spectra are provided in Figure A-1. Absorbance peaks were identified at wavelengths representing Nd and Sm like those during the loading and wash phases of the experiment. The evolution of the spectra as the rinse progresses are consistent with average effluent concentrations measured by ICP-MS, shown in Figure 3-1. There is not a significant shift in spectral features due to the changing acid and nitrate concentration.

4.0 Conclusions

DGA Resin was loaded to saturation with a representative Mk-18A feed simulant. A loading profile was developed, and the resin was determined to have a trivalent metal saturation capacity of 74 µmol/mL resin, including 68 µmol (~10 mg) of REEs/mL resin and 6 µmol of Fe/mL resin. However, the post-washing trivalent metal capacity of 68 µmol/mL resin represents the practical capacity of the resin for this process.

The saturation capacity determined in this work agrees with the literature but the Nd breakthrough point with REE loading of ~58 µmol/mL resin is lower than reported in a previous SRNL study. Lighter lanthanides breakthrough the resin well before the saturation capacity is reached. La through Nd breakthrough in order of increasing atomic number and Y was the strongest retained component by the resin. After processing 22.2 BV of feed through the column, similar to the amount estimated for the total process feed volume, the resin was loaded with REEs to 66 µmol/mL resin. At this point, 0% of Sm and 6% of Nd, surrogates for Cm and Am, respectively, broke through the resin bed.

Rinsing the saturated resin bed with 0.26 M HNO_3 was found to result in a rapid reduction of retention by the resin. After processing 2.8 BV of dilute acid rinse, the mean resin bed free acid concentration was reduced to 0.28 M and 3.1 BV of dilute acid rinse resulted in a reduction of the cumulative REE retention to 52 µmol/mL of resin. Like the loading behavior, lower atomic number lanthanides were the most readily desorbed components from the resin under dilute acid conditions. Estimating Cm and Am losses from the dilute acid rinse based on Sm and Nd losses, respectively, predicts that losses will be significant with excessive dilute acid rinse. Additionally, Sm may be more strongly retained by the resin than Cm, indicating that this approach could underpredict Cm losses. It is desired to minimize losses to no more than 5% of the maximum amount of Cm and Am contained in any quarter Mk-18A target to ensure compliance with high activity drain requirements. Based on Sm and Nd retention, it is estimated that 1.2 BV of dilute acid rinse would result in losses of 4.8% and 4.2% of the maximum amount of Cm and Am contained in a quarter target from saturated resin, respectively, and a mean resin bed free acid concentration of 1.8 M. Due to the non-conservative nature of this approach, 1 BV of dilute acid rinse may be a more appropriate target which results in estimated Cm and Am losses of 3.1% and 2.9% of the maximum amount contained in a quarter target from saturated resin, respectively, and a mean resin bed free acid concentration of 3.0 M. Recycle of the rinse effluent to the DGA feed tank is recommended so that it can be reprocessed with the next quarter target to further reduce losses.

The efficacy of real-time UV-vis spectroscopy for monitoring metals in effluents of dissolved Mk-18A material from DGA Resin was demonstrated. Significant absorption centered at *ca* 393 nm is attributed to Fe. Due to the weak retention of Fe and its lack of value for recovery, this feature is generally inconvenient as it interferes with identifying Sm absorption at *ca* 370 nm, but its evolution does provide some early insight to the loading progress. Of primary interest are features representing Nd, which provide a warning of forthcoming Am breakthrough. There is significant Nd contained in the Mk-18A targets, which is characterized by absorption at multiple wavelengths. A sharp and intense peak represents Nd at *ca* 578 nm which should be monitored for breakthrough as an early indicator that Am and Cm losses are imminent if additional feed is processed through the DGA column after Nd is observed to increase in the effluent.

5.0 References

(1) Robinson, S. M.; Benker, D. E.; Collins, E. D.; Ezold, J. G.; J. R, G.; Hogle, S. L. Production of Cf-252 and other transplutonium isotopes at Oak Ridge National Laboratory. *Radiochimica Acta* **2020**, *108* (9), 727-746. DOI: 10.1515/ract-2020-0008.
(2) Armstrong, C. R.; Brant, H. A.; Nuessle, P. R.; Hall, G.; Cadieux, J. R. Anthropogenic plutonium-244 in the environment: Insights into plutonium's longest-lived isotope. *Scientific Reports* **2016**, *6*, 21512. DOI: 10.1038/srep21512.
(3) Robinson, S. M.; Allender, J. S.; Patton, B. D. Processing and Disposition of Special Actinide Target Materials – 13138 In WM2013 Conference, Phoenix, Arizona; 2013.
(4) Ryan, J. L.; Wheelwright, E. J. Recovery and Purification of Plutonium by Anion Exchange. *Ind. Eng. Chem.* **1959**, *51*, 60-65. DOI: 10.1021/ie50589a038.
(5) Kyser, E. A. *Plutonium Loading onto Reillex HPQ Anion Exchange Resin*; WSRC-TR-2000-00372; Westinghouse Savannah River Company, 2001. DOI: 10.2172/773118.

(6) Karay, N. S.; Kyser, E. A.; Pierce, R. A. *Plutonium Purification by Anion Exchange for Mark-18A Target Processing*; SRNL-TR-2017-00193, Rev. 0; Savannah River National Laboratory, 2017.
(7) Zhu, Z.-X.; Sasaki, Y.; Suzuki, H.; Suzuki, S.; Kimura, T. Cumulative study on solvent extraction of elements by N,N,N′ ,N′ -tetraoctyl-3-oxapentanediamide (TODGA) from nitric acid into n-dodecane. *Analytica Chimica Acta* **2004**, *527* (2), 163-168. DOI: 10.1016/j.aca.2004.09.023.
(8) McCann, K. P.; Jones, M. A.; Kyser, E. A.; Smith, T. E.; Bridges, N. J. Scaling Trivalent Actinide and Lanthanide Recovery by Diglycolamide Resin from Savannah River Site's Mark-18A Targets. *Industrial & Engineering Chemistry Research* **2021**, *60* (1), 507-513. DOI: 10.1021/acs.iecr.0c03897.
(9) Horwitz, E. P.; McAlister, D. R.; Bond, A. H.; Barrans, R. E. Novel Extraction of Chromatographic Resins Based on Tetraalkyldiglycolamides: Characterization and Potential Applications. *Solvent Extraction and Ion Exchange* **2005**, *23* (3), 319–344. DOI: 10.1081/SEI-200049898.
(10) Nash, K. L. A comparison of new reagents and processes for hydrometallurgical processing of actinides. In Global 2001 international conference on: "back-end of the fuel cycle: from research to solutions", Paris, France; 2001.
(11) Gergoric, M.; Barrier, A.; Retegan, T. Recovery of Rare-Earth Elements from Neodymium Magnet Waste Using Glycolic, Maleic, and Ascorbic Acids Followed by Solvent Extraction. *Journal of Sustainable Metallurgy* **2019**, *5*, 85-96. DOI: 10.1007/s40831-018-0200-6.
(12) Pierce, R. A.; Karay, N. S. *Oxidation of DGA Resin for Mark-18A Fuel Processing*; SRNL-TR-2020-00184, Rev. 0; Savannah River National Laboratory, 2020.
(13) McCann, K. P.; Smith, T. E.; Jones, M. A.; Kyser, E. A.; Bridges, N. J. *Trivalent Actinide and Lanthanide Recovery from Mark-18A Targets by DGA Resin*; SRNL-STI-2019-000727, Rev. 0; Savannah River National Laboratory.
(14) Mills, M. S. *Mark-18A DGA Resin Drying and Decomposition Process: Testing Summary and Path Forward*; SRNL-L2250-2023-00002, Rev. 0; Savannah River National Laboratory, 2023.
(15) Chandran, K.; Venkatesan, K. A.; Anthonysamy, S.; Srinivasan, T. G. Thermal decomposition behaviour of diglycolamide - Nitric acid system. *Thermochimica Acta* **2014**, *583*, 59-66.
(16) Whittaker, D.; Geist, A.; Modolo, G.; Taylor, R.; Sarsfield, M.; Wilden, A. Applications of Diglycolamide Based Solvent Extraction Processes in Spent Nuclear Fuel Reprocessing, Part 1: TODGA. *Solvent Extraction and Ion Exchange* **2018**, *36* (3), 223-256. DOI: 10.1080/07366299.2018.1464269.
(17) Kyser, E. A. Mills, M. S., Ed.; Personal Communciation.
(18) Mills, M. S.; Kyser, E. A. *Research & Development Plan for Mark-18A DGA Low-Acid Rinse and Fluoride Decontamination Study*; SRNL-RP-2023-00400, Rev. 0; Savannah River National Laboratory, 2023.
(19) Lascola, R. J.; O'Rourke, P. E.; Kyser, E. A.; Immel, D. M.; Plummer, J. R.; Evans, E. V. *Spectrophotometers for plutonium monitoring in HB-Line*; SRNL-STI-2015-00454, Rev. 0; Savannah River National Laboratory, 2016.
(20) *DGA Resins*. Eichrom, 2023. https://www.eichrom.com/eichrom/products/dga-resins/ (accessed November 1, 2023).
(21) Tachimori, S.; Sasaki, Y.; Suzuki, S. Modification of TODGA-n-dodecane solvent with a monoamide for high loading of lanthanides(III) and actinides(III). *Solvent Extraction and Ion Exchange* **2002**, *20* (6), 687-699.
(22) McCann, K. P. *DGA Column Hot Test*; ELN Experiment ID J2101-00333-14; Savannah River National Laboratory, 2020.
(23) Dousma, J.; Bruyn, P. L. D. Hydrolysis-precipitation studies of iron solutions. I. Model for hydrolysis and precipitation from Fe(III) nitrate solution. *Journal of Colloid and Interface Science* **1976**, *56* (3), 527-539. DOI: 10.1016/0021-9797(76)90119-3.
(24) Rodden, C. J. Spectrophotometric determination of praseodymium, neodymium, and samarium. *Journal of Research of the National Bureau of Standards* **1941**, *26*, 557-570.
(25) Rodionova, O. Y.; Tikhomirova, T. I.; Pomerantsev, A. L. Spectrophotometric determination of Rare Earth Elements in aqueous nitric acid solutions for process control. *Analytica Chimica Acta* **2015**, *869*, 59-67. DOI: 10.1016/j.aca.2015.02.037.

(26) Franzen, P.; Gorter, J. P. M. W. C. J. Absorption of light in a solution of samarium nitrate. *Physica* **1943**, *10* (5), 365-368. DOI: 10.1016/S0031-8914(43)90023-0.
(27) Edlridge, H. W. *Estimation of Mark-18A Isotopic Inventories*; SRNL-L2200-2021-00037, Rev. 0; Savannah River National Laboratory, 2021.
(28) Geist, A.; Müllich, U.; Magnusson, D.; Kaden, P.; Modolo, G.; Wilden, A.; Zevaco, T. Actinide(III)/Lanthanide(III) Separation via Selective Aqueous Complexation of Actinides(III) using a Hydrophilic 2,5-Bis(1,2,4-Triazin-3-YL)-Pyridine in Nitric Acid. *Solvent Extraction and Ion Exchange* **2012**, *30* (5), 433-444. DOI: 10.1080/07366299.2012.671111.

Appendix A. Supplemental Information

Table A-1. Composite effluent cut volumes and compositions

Element	Cut ID							
	ECA	ECB	ECC	ECD	ECE	ECF	ECG	ECH
	Total volume of column effluent at end of cut (mL)							
	379	755	951	1150	1299	1402	1502	1602
	Total volume of column effluent at end of cut (BV)							
	8.86	17.7	22.2	26.9	30.4	32.8	35.1	37.5
	Concentration (mg/L)							
Cu	2.38E+01	2.59E+01	2.59E+01	2.58E+01	2.57E+01	2.58E+01	2.54E+01	2.55E+01
Fe	2.06E+02	2.76E+02	2.72E+02	2.60E+02	2.61E+02	2.51E+02	2.64E+02	2.54E+02
Sr	2.06E+02	2.76E+02	2.72E+02	2.60E+02	2.61E+02	2.51E+02	2.64E+02	2.54E+02
Y	4.57E+00	5.05E+00	5.03E+00	5.02E+00	5.08E+00	5.09E+00	5.02E+00	5.05E+00
La	< 1.00E-02	< 1.00E-02	< 1.00E-02	< 1.00E-02	< 1.00E-02	< 1.00E-02	< 1.00E-02	< 1.00E-02
Ce	< 1.00E-02	2.08E+01	5.97E+01	5.45E+01	4.40E+01	3.81E+01	3.50E+01	3.31E+01
Pr	< 1.00E-02	3.15E+01	1.29E+02	1.81E+02	1.56E+02	1.39E+02	1.30E+02	1.21E+02
Nd	< 1.00E-02	3.08E+00	1.93E+01	3.96E+01	3.96E+01	3.78E+01	3.66E+01	3.50E+01
Sm	< 1.00E-02	4.31E+00	3.95E+01	1.70E+02	2.41E+02	2.53E+02	2.70E+02	2.71E+02
Eu	< 1.00E-02	1.35E-02	1.95E-01	3.13E+00	1.29E+01	2.57E+01	3.53E+01	4.61E+01
Gd	< 1.00E-02	< 1.00E-02	< 1.00E-02	< 1.00E-02	3.18E-02	8.51E-02	1.38E-01	2.12E-01
Tb	< 1.00E-02	1.44E+00	4.20E+00	3.77E+00	3.10E+00	2.89E+00	2.89E+00	3.07E+00
Dy	< 1.00E-02	1.21E-02	8.99E-02	3.25E-01	4.34E-01	4.63E-01	4.69E-01	4.77E-01
Ho	< 1.00E-02	< 1.00E-02	2.08E-02	9.39E-02	1.41E-01	1.76E-01	1.96E-01	2.14E-01
Er	< 1.00E-02	< 1.00E-02	< 1.00E-02	3.31E-02	4.73E-02	5.38E-02	5.67E-02	5.81E-02
Tm	< 1.00E-02	< 1.00E-02	< 1.00E-02	< 1.00E-02	< 1.00E-02	< 1.00E-02	< 1.00E-02	< 1.00E-02
Yb	< 1.00E-02	< 1.00E-02	< 1.00E-02	< 1.00E-02	< 1.00E-02	< 1.00E-02	< 1.00E-02	< 1.00E-02
Lu	< 1.00E-02	< 1.00E-02	< 1.00E-02	< 1.00E-02	< 1.00E-02	< 1.00E-02	< 1.00E-02	< 1.00E-02

Table A-1. Composite effluent cut volumes and compositions

Element	Cut ID							
	ECI	ECJ	WC-1	WC-2A	WC-2B	WC-2C	WC-2D	WC-2E
	Total volume of column effluent at end of cut (mL)							
	1702	1812	1898	1925	1951	1978	2004	2030
	Total volume of column effluent at end of cut (BV)							
	39.8	42.4	44.4	45.0	45.6	46.2	46.9	47.5
	Concentration (mg/L)							
Cu	2.53E+01	2.53E+01	1.07E+01	1.53E-01	8.19E-02	3.07E-02	1.32E-02	1.76E-02
Fe	2.54E+02	2.58E+02	9.41E+01	<1.00E-01	<1.00E-01	<1.00E-01	<1.00E-01	<1.00E-01
Sr	2.54E+02	2.58E+02	9.41E+01	<1.00E-01	<1.00E-01	<1.00E-01	<1.00E-01	<1.00E-01
Y	5.06E+00	5.03E+00	1.91E+00	3.27E-02	2.04E-02	< 1.00E-02	< 1.00E-02	< 1.00E-02
La	< 1.00E-02	< 1.00E-02	< 1.00E-02	< 1.00E-02	6.45E-02	1.26E-01	8.53E-02	6.25E-02
Ce	3.17E+01	3.10E+01	1.47E+01	1.46E+00	4.47E-01	2.87E-01	2.18E-01	1.80E-01
Pr	1.12E+02	1.06E+02	5.38E+01	1.90E+01	1.97E+01	2.12E+01	1.43E+01	9.74E+00
Nd	3.33E+01	3.14E+01	1.91E+01	8.00E+00	2.17E+01	2.57E+01	1.56E+01	1.04E+01
Sm	2.72E+02	2.70E+02	1.52E+02	6.54E+01	4.06E+02	4.53E+02	2.54E+02	1.58E+02
Eu	5.91E+01	7.28E+01	5.09E+01	2.31E+01	3.78E+02	3.82E+02	1.81E+02	1.12E+02
Gd	3.21E-01	4.44E-01	3.83E-01	1.73E-01	3.64E+00	4.00E+00	2.02E+00	1.27E+00
Tb	3.48E+00	4.17E+00	3.05E+00	1.11E+00	2.87E+01	3.56E+01	1.95E+01	1.35E+01
Dy	4.71E-01	4.67E-01	2.82E-01	1.23E-01	8.59E-01	1.02E+00	5.90E-01	3.94E-01
Ho	2.33E-01	2.54E-01	1.64E-01	7.30E-02	8.04E-01	8.54E-01	4.46E-01	2.82E-01
Er	5.97E-02	6.16E-02	3.80E-02	1.64E-02	1.32E-01	1.44E-01	7.79E-02	5.05E-02
Tm	< 1.00E-02	< 1.00E-02	< 1.00E-02	< 1.00E-02	4.29E-02	4.38E-02	2.17E-02	1.34E-02
Yb	< 1.00E-02	1.51E-02	1.55E-02	< 1.00E-02	2.18E-01	2.71E-01	1.50E-01	9.52E-02
Lu	< 1.00E-02	< 1.00E-02	< 1.00E-02	< 1.00E-02	< 1.00E-02	< 1.00E-02	< 1.00E-02	< 1.00E-02

- "ECx" represents a feed raffinate cut; "WC-1" represents the 8 M HNO_3 wash; "WC-2x" represents a dilute acid rinse cut.

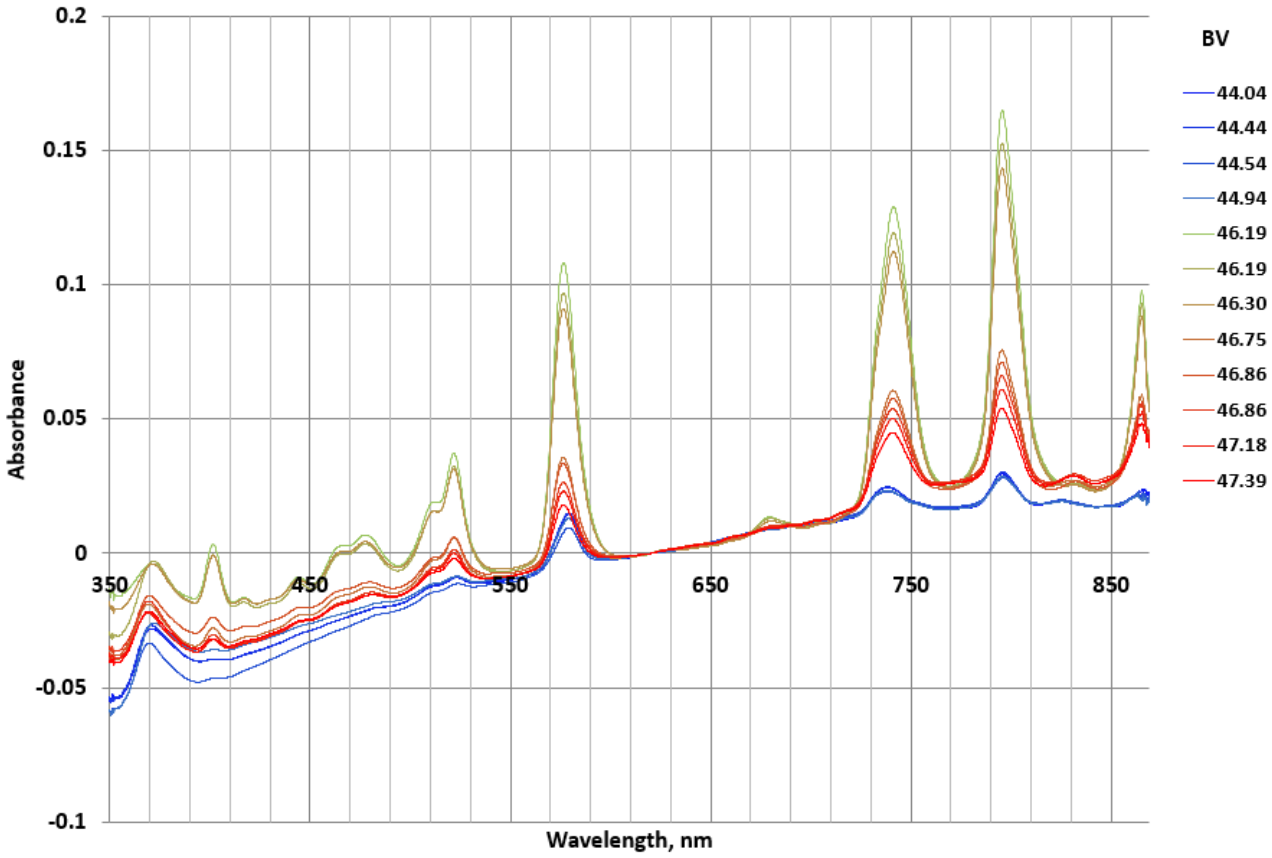

Figure A-1. Absorption spectral evolution during dilute HNO_3 rinse

Spectrometer Details

The spectroscopy system comprises of instruments hardware and a software control system. The hardware system includes:

- Avantes Multichannel Spectrophotometer AVS-RACKMOUNT-USB2
- Avantes spectrophotometer: AS60014U21, AS60015U21
- Optical beam combiner/splitter BSC-DA-SRNL1
- Xenon arc lamp AVALIGHT-XE-HP
- Tungsten-Halogen lamp AVALIGHT-HAL
- Fiber optic cables – Multimode fibers, 400 micron high-OH core, 0.22 na
- Computer with USB Interface
- COTS assembled 90mm Stainless steel flow cell. Swagelok #SS-2000-3
- COTS collimator, Edmund Optics #88-173

The instrument control software system is a control program written in the Visual Basic environment.

- Hardware interface program VB_App_AS7010.EXE
  - *To configure and communicate with Avantes spectrophotometers*.
- Spectroscopic data processing and analysis program Avantes_Model_E.XLSM workbook
  - *Convert raw intensity signals to corrected spectra and other useful materials characteristics*.

Distribution:

christopher.armstrong@srnl.doe.gov
christopher.orton@srnl.doe.gov
drew.fairchild@srnl.doe.gov
eddie.kyser@srnl.doe.gov
frank.pennebaker@srnl.doe.gov
gregg.morgan@srnl.doe.gov
harris.eldridge@srnl.doe.gov
jarrod.gogolski@srnl.doe.gov
john.auxier@srnl.doe.gov
jonathan.duffey@srnl.doe.gov
kathryn.taylor-pashow@srnl.doe.gov
matthew.mills@srnl.doe.gov
matthew02.williams@srnl.doe.gov
rebecca.carter@srnl.doe.gov
robert.pierce@srnl.doe.gov
samuel.uba@srnl.doe.gov
sasha.mills@srnl.doe.gov
tracy.rudisill@srnl.doe.gov
william02.king@srnl.doe.gov